Uncertainty Quantification of Printed Microwave Interconnects by Use of the Sparse Polynomial Chaos Expansion Method

Aristeides D. Papadopoulos, *Member, IEEE*, Bijan K. Tehrani, *Member, IEEE*, Ryan A. Bahr, *Member, IEEE*, Emmanouil M. Tentzeris, *Fellow, IEEE*, and Elias N. Glytsis, *Senior Member, IEEE*

***Abstract*— The performance of printed RF interconnect structures for microwave applications is highly dependent on their geometric characteristics as well as manufactured pattern fabrication errors/variations, that can only be insufficiently modeled by current simulation techniques. Here, for the first time, the response of such systems is accurately investigated when random fabrication errors are introduced in the geometric-design variables. To analyze these structures in a computationally efficient way, sparse-basis-polynomial-chaos-expansions (SB-PCE) are used to approximate the quantities of interest using a limited number (sparse) of basis functions. The size of the PCE series is reduced by retaining the most important terms. These are computed using the orthogonal-matching-pursuit algorithms from compressed-sensing (CS). In CS, a relatively small number of deterministic model evaluations is needed and a sparse but reliable PCE is found. The SB-PCE method is proven accurate and much more efficient (roughly two orders of magnitude shorter execution time) compared to alternative methods such as the Monte-Carlo (MC) and least-squares-PCE (LS-PCE) enabling for the first time the accurate modeling of realistic RF structures for specific manufacturing process variations. Numerical results for a monolithic-microwave-integrated circuit (MMIC) verify the effectiveness of the method and describes the structure's performance under uncertainty.**

***Index Terms*— Compressed sensing (CS), polynomial chaos, RF-interconnects, uncertainty.**

I. Introduction

THE system-in-package (SiP) approach to microwave packaging focuses on the integration of multiple integrated circuit (IC) devices, passive components, and other wireless system peripherals all within a single package. The elimination of discrete component packages allows for a higher degree of system miniaturization while promoting an improvement in system efficiency through the reduction of module-to-module interconnection losses, especially within the millimeter-wave (mm-wave) wireless regime. In a SiP configuration, first-level interconnects are required to interface IC dies with the circuitry on their host packaging substrate. These first-level interconnects are traditionally achieved through thermosonic bonding techniques for surface mount configurations. However, these methods can suffer from high parasitic losses at mm-wave frequencies [1]. Recent efforts in the development of first-level interconnects for mm-wave wireless systems are reaching beyond traditional RF laminate stacks and standard wire/ribbon bonding approaches to investigate additive manufacturing techniques, specifically inkjet and aerosol jet printing [2]–[4].

Manufacturing processes for RF structures including lithography, milling, and additive techniques all contain inherent tolerances, which consequentially lead to patterning errors and therefore induce uncertainty in their performance. A popular method for uncertainty quantification (UQ) is the polynomial chaos expansion (PCE) model [5]. PCEs produce reliable results efficiently, compared to the Monte-Carlo (MC) method [6]. However, PCEs can become computationally expensive when the number of random inputs increases and/or when the quantities of interest (QoI) that are required in the process, are computationally demanding (e.g., when full-wave solvers are used), which commonly happens with printed RF structures. There are various solutions for cases that the PCE computational cost becomes significant. Modified truncation schemes of the PCE series can be applied such as hyperbolic [7] or hyperbolic-cross indices [8]. In addition, methods from compressed sensing (CS) have been used in PCE to construct sparse models which require smaller number of QoI evaluations.

In this study, as a proof-of-concept demonstration, a sparse PCE model is constructed for the UQ of S-parameters (QoI) of microwave interconnects. First, a reduced number of basis functions is used in the PCE via application of the hyperbolic truncation scheme. Then, a sparse vector of PCE coefficients is recovered by CS, using a minimal number of deterministic evaluations of the QoI. The QoI's are calculated by a full-wave finite-element method (FEM) solver. Therefore, methods such as the MC or the least square (LS)-PCE which require significant large number of QoI's are not efficient. In particular, the simple and effective orthogonal matching pursuit (OMP) [9] algorithm is used for the coefficients vector recovery. At the end of this work, numerical tests are

Manuscript received September 2, 2021; accepted September 21, 2021. Date of publication October 6, 2021; date of current version January 10, 2022. This work was supported in part by the Northrop Grumman, in part by the NSF, and in part by the Air Force Research Laboratory (AFRL). *(Corresponding author: Aristeidis D. Papadopoulos.)*

Aristeides D. Papadopoulos and Elias N. Glytsis are with the School of Electrical and Computer Engineering, National Technical University of Athens, 15780 Athens, Greece (e-mail: arpapad@mail.ntua.gr).

Bijan K. Tehrani, Ryan A. Bahr, and Emmanouil M. Tentzeris are with the School of Electrical and Computer Engineering, Georgia Institute of Technology, Atlanta, GA 30332 USA (e-mail: etentze@ece.gatech.edu).

Color versions of one or more figures in this letter are available at https://doi.org/10.1109/LMWC.2021.3115618.

Digital Object Identifier 10.1109/LMWC.2021.3115618

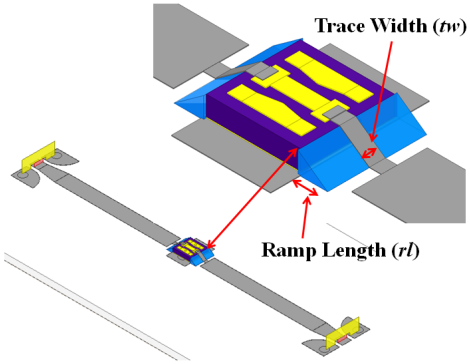

Fig. 1. Geometry of an mm-wave interconnect. The geometric uncertain parameters ramp length (*rl*) and trace width (*tw*) are shown.

presented and the accurate estimation of the impact of the manufacturing-induced geometric uncertain variables on the QoI is highlighted.

II. Sparse Basis PCE

In this work, printed mm-wave interconnect structures, such as the ramp structure shown in Fig. 1, are analyzed under uncertain geometric parameters. In particular, the ramp length (*rl*) and trace width (*tw*) are considered uniformly distributed random variables with real-world variations induced from printed circuit manufacturing techniques.

In general, if y is the QoI that depends on the frequency f and $\boldsymbol{\xi} \equiv [\xi_1, \xi_2, \ldots, \xi_d]$ is the vector of random variables, the QoI is approximated by the following expansion (PCE) [5]:

$$y(f, \boldsymbol{\xi}) \cong \sum_{\boldsymbol{\alpha} \in A_p} c_{\boldsymbol{\alpha}}(f) \Psi_{\boldsymbol{\alpha}}(\boldsymbol{\xi}) \tag{1}$$

where $\boldsymbol{\alpha} \equiv (a_1, a_2, \ldots, a_d) \in \mathbb{N}_0^d$, $c_{\boldsymbol{\alpha}}(f)$ are the expansion coefficients and are $\Psi_{\boldsymbol{\alpha}}(\boldsymbol{\xi})$ the basis functions of the PCE. The basis functions are given as $\Psi_{\boldsymbol{\alpha}}(\boldsymbol{\xi}) = \prod_{i=1}^{d} \psi_{\alpha_i}(\xi_i)$ (assuming that ξ_i are independent) where $\psi_{\alpha_i}(\xi_i)$ is the Legendre polynomial of order α_i. Legendre polynomials are chosen for optimum convergence of the PCE series when the ξ_i's are uniformly distributed [5]. It is noted that alternative choices for the polynomial and the random variable distribution exist that lead to optimal convergence [5]. The index vector $\boldsymbol{\alpha}$ belongs to the set $A_p = \{\boldsymbol{\alpha}: ||\boldsymbol{\alpha}||_1 \leq p\}$, where $||\cdot||_1$ is the l_1-norm. Therefore, the polynomials $\Psi_{\boldsymbol{\alpha}}(\boldsymbol{\xi})$ in the PCE series have total degree smaller or equal to p (total-degree truncation scheme). The cardinality of A_p is $|A_p| = (p+d)!/(p!d!)$.

In PCE methods, the "*sparsity-of-effects*" principle holds implying that the QoI of the structure depends mainly on low-order polynomial interactions. Therefore, a reduction in the number of terms in the PCE can be applied. Based on this, the hyperbolic index set [8] is defined as $A_p^q = \{\boldsymbol{\alpha}: ||\boldsymbol{\alpha}||_q \leq p\}$, $||\cdot||_q$ is the q-quasi-norm [7]

$$\|\boldsymbol{\alpha}\|_q \equiv \left(\sum_{i=1}^{d} \alpha_i^q \right)^{1/q} \tag{2}$$

where $0 < q < 1$. It is noted that the index set, A_p^q, should balance between accuracy (keep important terms) and computational cost (keep the total number of terms to a minimum).

CS is a research field in signal processing [10], where a sparse signal is recovered from a reduced number of measurements (or QoI). Recently CS has been applied in PCE [11], [12] where a sparse PCE can be derived with smaller number of model evaluations than the number of basis functions. This could be a very effective approach especially when the model QoI evaluations require computationally demanding and often unrealistically high number of time-consuming simulations.

In particular, $N(< M \equiv |A_p^q|)$ number of random points $\boldsymbol{\xi}^{(1)}, \ldots, \boldsymbol{\xi}^{(N)}$ is selected and the l_0 optimization problem is solved

$$\mathbf{c}^* = \arg_{\mathbf{c}} \min \|\mathbf{c}\|_0 \quad \text{s.t. } \boldsymbol{\Psi}\mathbf{c} = \boldsymbol{y} \tag{3}$$

where $\mathbf{c}$ is the vector of PCE coefficients, $\boldsymbol{\Psi} \in \mathbb{R}^{N \times M}$ is a matrix with elements $\boldsymbol{\Psi}_{i,j} = \Psi_j(\boldsymbol{\xi}^{(i)})$, $\boldsymbol{y} = [y(\boldsymbol{\xi}^{(1)}), \ldots, y(\boldsymbol{\xi}^{(N)})]$, and $||\mathbf{c}||_0$ is the l_0 norm of $\mathbf{c}$. The vector $\mathbf{c}^*$ is estimated by use of the OMP algorithm. OMP is a greedy algorithm that iteratively finds the columns of $\boldsymbol{\Psi}$ that participate in the creation of $\mathbf{y}$. For a $\mathbf{c}^*$ recovery of s nonzero coefficients, there will be s-iterations in the OMP. Alternatively, the iterations continue until the residual (i.e., $|\boldsymbol{\Psi}\boldsymbol{c}^{(i)} - \boldsymbol{y}|$), at the ith OMP iteration, is smaller than a given error level (ε). Another approach to specify the PCE coefficients is to solve

$$\mathbf{c}^* = \arg_{\mathbf{c}} \min \|\mathbf{c}\|_2 \quad \text{s.t. } \boldsymbol{\Psi}\mathbf{c} = \boldsymbol{y} \tag{4}$$

where the solution $\mathbf{c}^*$ is the LS solution of $\boldsymbol{\Psi}\mathbf{c} = \mathbf{y}$, but with the number of random points N being usually between $2M$ and $5M$. The LS-PCE, SB-PCE solutions are compared in Section III.

III. Numerical Results

In order to investigate the effects of fabrication uncertainties for printed techniques with SiP assembly approaches, a ramp interconnect configuration is selected for evaluation. The design targets the interconnection of a Ka-band GaAs 0 dB attenuator (RF-thru) monolithic microwave IC (MMIC) with a 6.6 mil Rogers 4350 host substrate in a surface-mount configuration. Ground-signal-ground coplanar waveguide (CPW) to microstrip transitions is included to enable potential probe-based characterization, patterned with silver nanoparticle (SNP) ink. The ramp interconnects are realized through the printing of SU-8 polymer dielectric ramp structures and the subsequent patterning of SNP metallic transitions, similar to the process outlined in [2]. Fig. 1 shows the high frequency structure simulator (HFSS) model of the printed interconnect test vehicle, with a detailed image highlighting the physical parameters to be investigated (*tw, rl*). The (*tw, rl*) variables are uniformly distributed with average values (80, 150) μm and a 10% (common experimental values) variation. The QoI are the $|S_{11}|$, $|S_{21}|$ parameters (absolute values are used but the structure is passive thus $S_{11}, S_{21} < 0$) which are computed with the *very accurate* HFSS FEM fullwave solver. Therefore, very accurate phase values can also

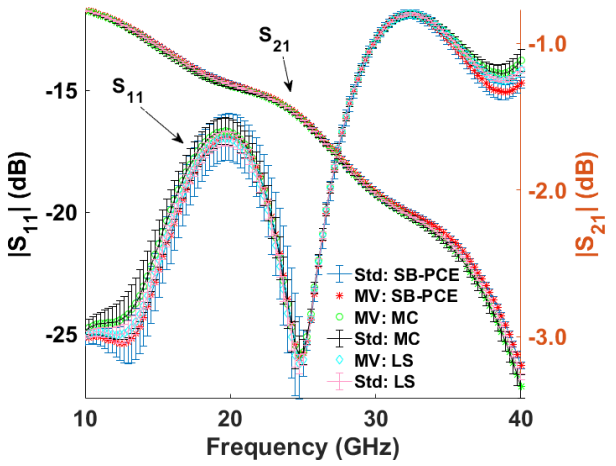

Fig. 2. MV and Std of the $|S_{11}|$ (right), $|S_{21}|$ (left), parameters for 10% uncertainty, calculated by the SB-PCE, LS-PCE, and MC methods.

TABLE I
COMPARISON OF THE SB-PCE, LS-PCE, AND MC METHODS

ME(.):V≡mean(|MC(.)-V(.)|)/max(|V(.)|)	MV	Std	N
ME(S_{11}):SB-PCE	0.0153	0.1122	4
ME(S_{11}):LS-PCE	0.0100	0.4297	48
ME(S_{21}):SB-PCE	0.0092	0.3742	4
ME(S_{21}):LS-PCE	0.0039	0.5725	48

be obtained and similarly their uncertainty can be quantified. Indeed the mean value (MV) and the standard deviation (Std) of the S_{11}, S_{21} phases have been calculated but since the Std in all cases was very small, the UQ analysis of the phases is insignificant and will not be analyzed further. In Fig. 2, the MV and Std of $|S_{11}|$, $|S_{21}|$ are shown, computed from the SB-PCE, LS-PCE (for $N = 4M$) and are compared to the corresponding MC values in the frequency range: 10–40 GHz. In all numerical results, $q = 0.75$, $p = 4$, for the A_p^q hyperbolic index sets. These values of q and p were chosen empirically. Alternatively, adaptive PCE schemes [7] could be used, but these are usually applied for higher dimensional problems. After the PCE coefficients are specified, the MV of the QoI (y) is MV $= c_0$ and the variance is computed as

$$\sigma^2\{y\} \cong \sum_{\boldsymbol{\alpha} \in A_4^{0.75} - \{\mathbf{0}\}} c_{\boldsymbol{\alpha}}^2 \|\Psi_{\boldsymbol{\alpha}}(\boldsymbol{\xi})\|^2. \quad (5)$$

A very good agreement is observed between the MC and the SB-PCE results, for the chosen total polynomial order $p = 4$.

In Table I, the Mean(in frequency)-Error (ME) between the SB-PCE, LS-PCE methods and the MC reference results are shown along where the number of model evaluations N. It is observed that the SB-PCE and LS-PCE methods have the smaller Std and MV Mean Error, respectively. However, SP-PCE is more computationally efficient than LS-PCE since the former requires $N < M$ number of measurements, while the latter requires $N = 4M$. It is noted that for the two-uncertain-variable case, when $p = 4$, there are 17 polynomials in the PCE, which are reduced to 12 by the hyperbolic truncation. In the SB-PCE case, only four model evaluations were used and the OMP was iterated until the residual was smaller than $\varepsilon = 10^{-6}$ which resulted in keeping just four nonzeros PCE coefficients. On the other hand, 200 model evaluations were used in the MC case. Considering that each evaluation by HFSS lasted ∼5 min the run time for each subfigure in Fig. 2 was 20 min for the SB-PCE, compared to 17 h for the MC!. From the PCE coefficients, the Sobol total (ST) sensitivity indices can be calculated for each uncertain variable *tw, rl*. The ST indices importance is that they quantify the contribution of each random variable to the uncertainty of the QoI (y). In particular, ST_i expresses the percentage of the ith uncertain variable in the variance of $y = \{|S_{11}|, |S_{21}|\}$. It is given by

$$ST_i = \frac{\sum_{\boldsymbol{\alpha} \in I_i} c_{\boldsymbol{\alpha}}^2 \|\Psi_{\boldsymbol{\alpha}}(\boldsymbol{\xi})\|^2}{\sigma^2\{\mathbf{y}\}}, \quad I_i = \{\mathbf{a} \in \mathbb{N}^d, a_i > 0\}. \quad (6)$$

The ST_i's, $i = \{tw, rl\}$ as a function of the operation frequency of the device, are shown in Fig. 3. It is observed that for both QoI's, $\{|S_{11}|, |S_{21}|\}$ and for all frequencies, $ST_{tw} > ST_{rl}$. Therefore, the QoI's uncertainty is mainly due to the *tw* variable, and for most frequencies, it is insensitive to the *rl* variable ($ST_{rl} \approx 0$).

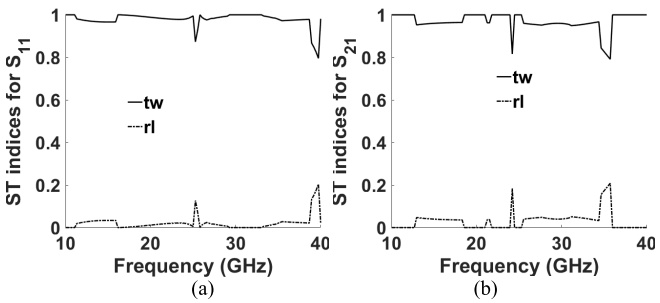

Fig. 3. ST indices of the *tw*, *rl* uncertain design variables for (a) $|S_{11}|$ and (b) $|S_{21}|$.

IV. CONCLUSION

Here, the performance of a printed mm-wave ramp interconnect configuration has been studied, considering stochastic geometric design parameters with manufacturing induced dimension variations typical with standard printed circuit fabrication technologies. Reliable ultra sparse, PC expansions of the S_{11}, S_{21} parameters have been constructed by combining the hyperbolic truncation scheme and the OMP algorithm. The developed SB-PCE method is sufficiently accurate and dramatically more computationally efficient (approximately two-orders run time) than the LS-PCE and MC methods. Our results feature an accurate estimation of the impact of geometric uncertainties on the S-parameters and overall performance in the bandwidth of interest, that would be critical for the reliable assessment of a system's sensitivity to tolerances with the geometry of its printed RF circuitry, especially for broadband 5G/B5G mmW applications. Similarly, additional uncertain variables (uv) can be considered such as line edge roughness, thickness and resistivity variations, coffee ring effects, scalloping, bulging, drop displacement, satellites cleanliness, and wetting variations. Future extensions will entail studies of additional uv and more challenging configurations, e.g., a Luneburg lens gradient material [13].

REFERENCES

[1] Y. P. Zhang and D. Liu, "Antenna-on-chip and antenna-in-package solutions to highly integrated millimeter-wave devices for wireless communications," *IEEE Trans. Antennas Propag.*, vol. 57, no. 10, pp. 2830–2841, Oct. 2009.

[2] B. K. Tehrani and M. M. Tentzeris, "Fully inkjet-printed ramp interconnects for wireless Ka-band MMIC devices and multi-chip module packaging," in *Proc. 48th Eur. Microw. Conf. (EuMC)*, Sep. 2018, pp. 1037–1040.

[3] X. He, B. K. Tehrani, R. Bahr, W. Su, and M. M. Tentzeris, "Additively manufactured mm-wave multichip modules with fully printed 'smart' encapsulation structures," *IEEE Trans. Microw. Theory Techn.*, vol. 68, no. 7, pp. 2716–2724, Jul. 2020.

[4] M. T. Craton, X. Konstantinou, J. D. Albrecht, P. Chahal, and J. Papapolymerou, "A chip-first microwave package using multimaterial aerosol jet printing," *IEEE Trans. Microw. Theory Techn.*, vol. 68, no. 8, pp. 3418–3427, Aug. 2020.

[5] D. Xiu and G. E. Karniadakis, "The Wiener–Askey polynomial chaos for stochastic differential equations," *SIAM J. Sci. Comput.*, vol. 24, no. 2, pp. 619–644, Jul. 2002.

[6] C. P. Robert, *Monte Carlo Methods*. Hoboken, NJ, USA: Wiley, 2014.

[7] G. Blatman, "Adaptive sparse polynomial chaos expansions for uncertainty propagation and sensitivity analysis," Ph.D. dissertation, Inst. Français Mecanique Avancee, Univ. Blaise Pascal, Clermont-Ferrand, France, 2009.

[8] J. Shen and L.-L. Wang, "Sparse spectral approximations of high-dimensional problems based on hyperbolic cross," *SIAM J. Numer. Anal.*, vol. 48, no. 3, pp. 1087–1109, 2010.

[9] J. A. Tropp and A. C. Gilbert, "Signal recovery from random measurements via orthogonal matching pursuit," *IEEE Trans. Inf. Theory*, vol. 53, no. 12, pp. 4655–4666, Dec. 2007.

[10] D. L. Donoho, "Compressed sensing," *IEEE Trans. Inf. Theory*, vol. 52, no. 4, pp. 1289–1306, Apr. 2006.

[11] J. Hampton and A. Doostan, "Compressive sampling of polynomial chaos expansions: Convergence analysis and sampling strategies," *J. Comput. Phys.*, vol. 280, pp. 363–386, Jan. 2015.

[12] L. Guo, A. Narayan, and T. Zhou, "A gradient enhanced l_1-minimization for sparse approximation of polynomial chaos expansions," *J. Comput. Phys.*, vol. 367, pp. 49–64, Aug. 2018.

[13] R. A. Bahr, A. O. Adeyeye, S. Van Rijs, and M. M. Tentzeris, "3D-printed omnidirectional Luneburg lens retroreflectors for low-cost mm-wave positioning," in *Proc. IEEE Int. Conf. RFID*, Orlands, FL, USA, Sep. 2020, pp. 1–7.